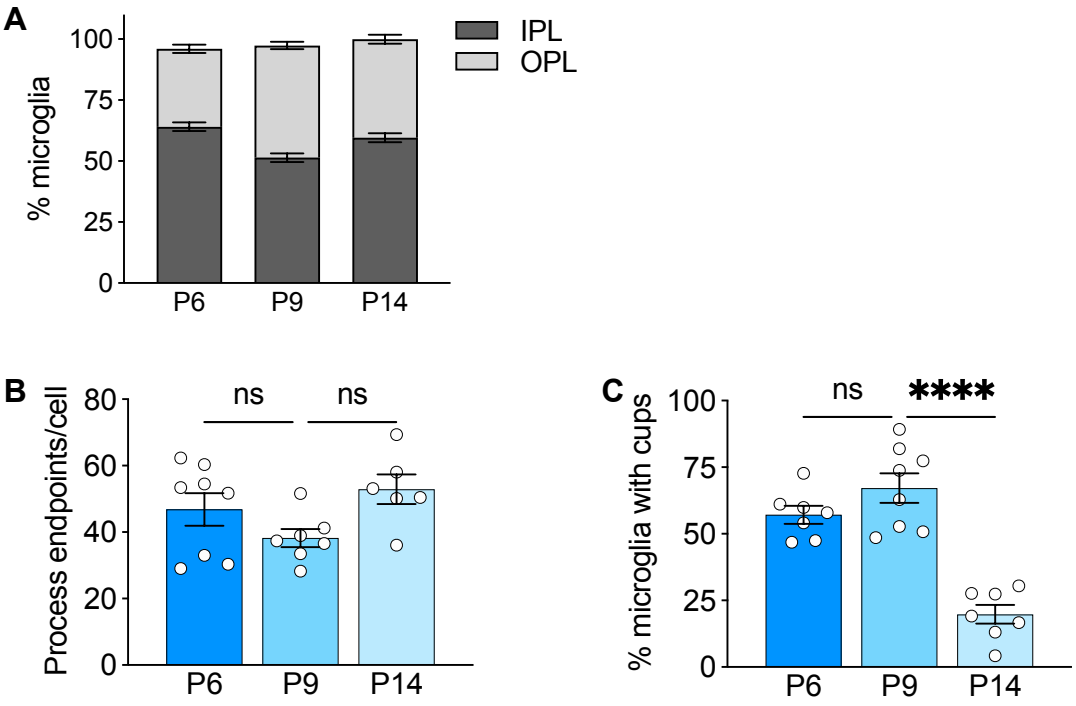

Figure S1. Microglia localization to synapse layers coincided with synapse emergence, Related to Figure 1

(**A**) Quantification of microglia spatial distribution between the inner plexiform (IPL) and outer plexiform (OPL) layers at P6, P9, and P14. n=3 mice for P6, n=4 for P9, n=4 for P14.

(**B**) Quantification of process endpoints per microglia at P6, P9, and P14 in WT retinas. n=8 mice for P6, n=7 for P9, n=6 for P14, one-way ANOVA with posthoc Bonferroni correction.

(**C**) Quantification of percent microglia with phagocytic cups at P6, P9, and P14 in WT retinas. n=7 for P6, n=8 for P9, n=7 for P14, one-way ANOVA with posthoc Bonferroni correction.

Data were pooled from two to three independent experiments. All data are presented as the mean ± SEM. ****p<0.0001, ns, not significant.

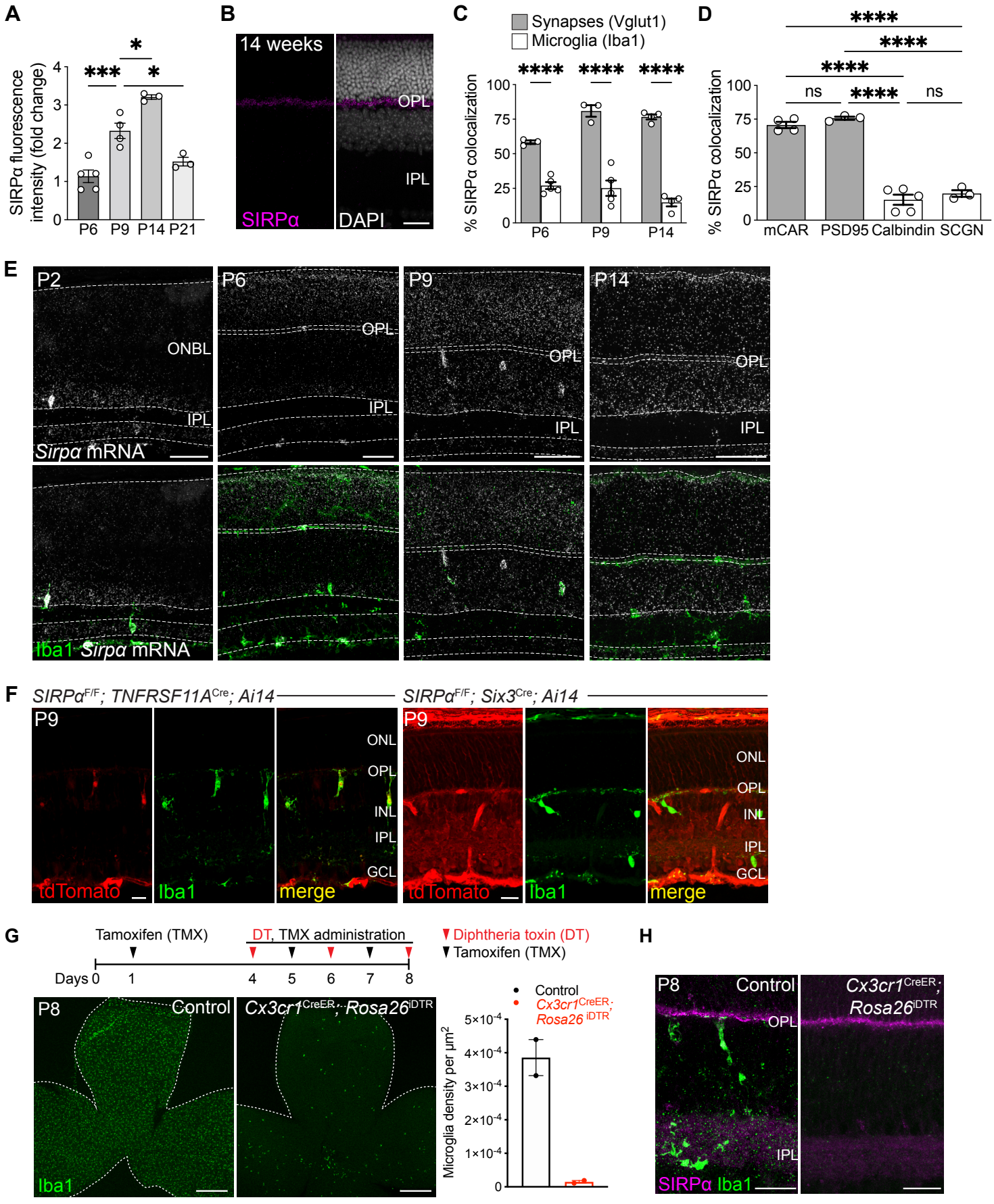
A
SIRPα fluorescence intensity (fold change)
P6 P9 P14 P21
B
14 weeks
OPL
IPL
SIRPα
DAPI
C
Synapses (Vglut1)
Microglia (Iba1)
% SIRPα colocalization
P6 P9 P14
D
% SIRPα colocalization
mCAR PSD95 Calbindin SCGN
ns
E
P2 P6 P9 P14
ONBL
OPL
IPL
Sirpα mRNA
Iba1 Sirpα mRNA
F
SIRPα F/F; TNFRSF11A Cre; Ai14
SIRPα F/F; Six3 Cre; Ai14
ONL
OPL
INL
IPL
GCL
tdTomato
Iba1
merge
G
Tamoxifen (TMX)
DT, TMX administration
Diphtheria toxin (DT)
Tamoxifen (TMX)
Days 0 1 4 5 6 7 8
P8 Control
Cx3cr1 CreER; Rosa26 iDTR
Microglia density per µm2
H
P8 Control
Cx3cr1 CreER; Rosa26 iDTR
SIRPα Iba1

Figure S2. Neurons produced the majority of SIRPα, Related to Figures 2, 3.
(**A**) Quantification of the mean SIRPα fluorescence intensity in OPL at P6, P9, P14 and P21 in WT mice. n=5 for P6, n=4 for P9, n=3 for P14, n=3 for P21. Data were compared using two-way ANOVA with posthoc Bonferroni correction.
(**B**) Representative confocal image showing SIRPα expression (magenta) in the OPL at 14 weeks. Scale bars, 25 μm.
(**C**) Quantification of the degree of colocalization between SIRPα and synapses (Vglut1) or microglia (Iba1) in P6, P9, and P14 WT retinas using Manders' coefficients (MCC). n=3 per timepoint for Vglut1, n=4 per timepoint for Iba1 quantifications. Data were compared using two-way ANOVA with posthoc Bonferroni correction.
(**D**) Quantification of the degree of colocalization between SIRPα and presynaptic markers (mCAR for cone terminals, PSD95 for rod terminals) or postsynaptic markers (Calbindin for horizontal cell dendrites, SCGN for cone bipolar cell dendrites) in P14 WT retinas using Manders' coefficients (MCC). n=4 for mCAR, n=3 for PSD95, n=5 for Calbindin, and n=3 for SCGN. Data were compared using two-way ANOVA with posthoc Bonferroni correction.
(**E**) Representative fluorescence in situ hybridization (RNAscope) images of SIRPα and microglia marker Iba1 in P2, P6, P9, and P14 WT retinas. Scale bars, 50 μm.
(**F**) Representative confocal images of tdTomato expression (red) upon Cre activity in P9 *SIRPα*$^{F/F}$; *TNFRSF11A*^{Cre}; *Ai14* and *SIRPα*$^{F/F}$; *Six3*^{Cre}; *Ai14* retinas stained with microglia marker Iba1 (green). Scale bars, 10 μm.
(**G**) Microglia ablation paradigm. Tamoxifen (TMX) and diphtheria toxin (DT) were administrated at the indicated times (top). Representative confocal images and quantification of microglia number in P8 wholemount *Cx3cr1*^{CreER}; *Rosa26*^{iDTR} and control retinas. This model depleted the majority (~96%) of microglia in P8 retinas.
(**H**) Representative confocal images of SIRPα staining (magenta) in P9 *Cx3cr1*^{CreER}; *Rosa26*^{iDTR} and control retinas stained with microglia marker Iba1 (green). Scale bars, 25 μm.
Data in (**A**) to (**D**) were pooled from 2-3 independent experiments. Data in (**G**) were obtained from one experiment. All data are presented as the mean ± SEM. *p<0.05, ***p<0.001, ****p<0.0001, ns, not significant.

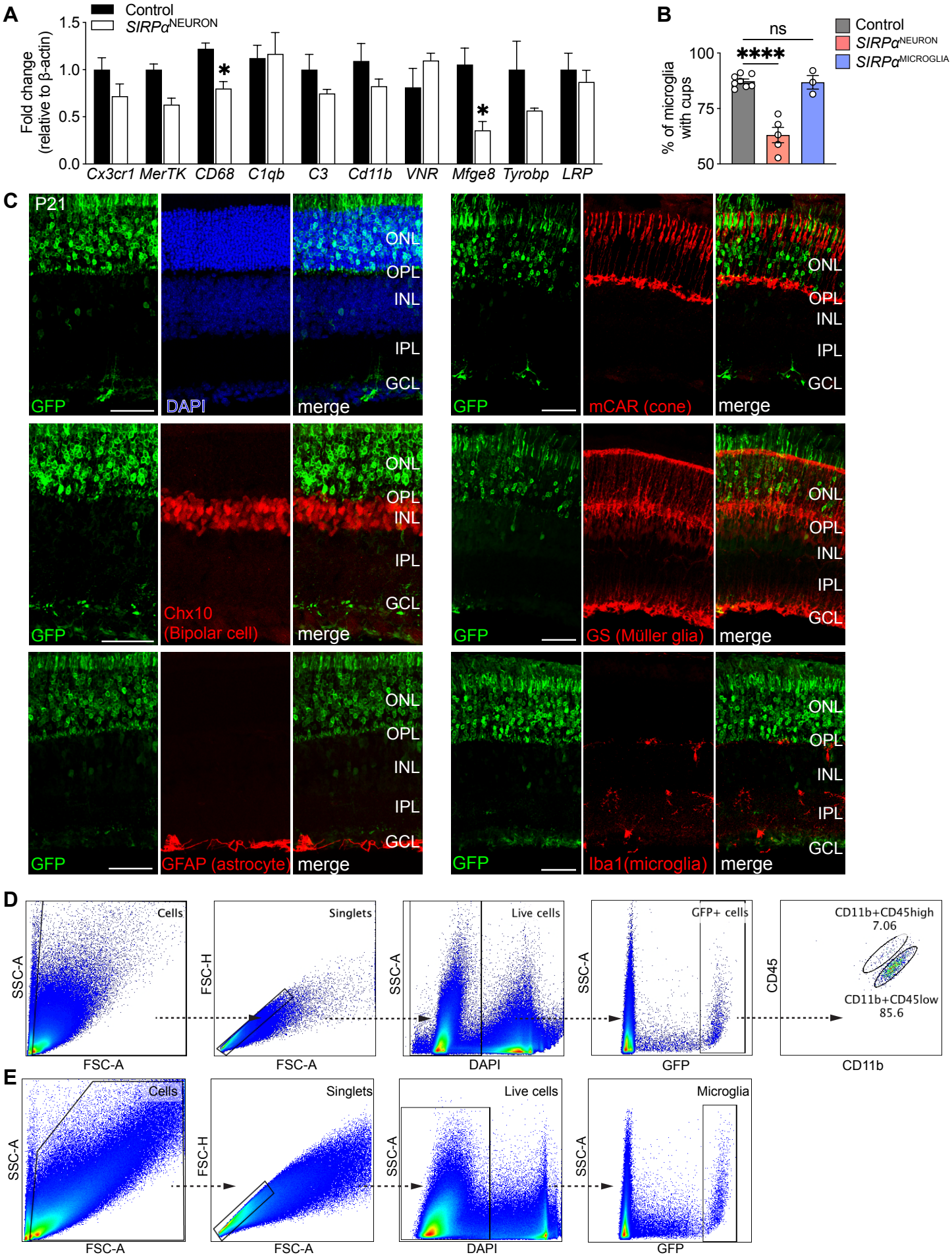
A
Control
SIRPα NEURON
Fold change (relative to β-actin)
1.5
1.0
0.5
0.0
*
*
Cx3cr1
MerTK
CD68
C1qb
C3
Cd11b
VNR
Mfge8
Tyrobp
LRP
B
Control
SIRPα NEURON
SIRPα MICROGLIA
ns
****
% of microglia with cups
100
75
50
C
P21
GFP
DAPI
merge
mCAR (cone)
Chx10 (Bipolar cell)
GS (Müller glia)
GFAP (astrocyte)
Iba1(microglia)
ONL
OPL
INL
IPL
GCL
D
Cells
Singlets
Live cells
GFP+ cells
CD11b+CD45high
7.06
CD11b+CD45low
85.6
SSC-A
FSC-A
FSC-H
DAPI
GFP
CD45
CD11b
E
Cells
Singlets
Live cells
Microglia
SSC-A
FSC-A
FSC-H
DAPI
GFP

Figure S3. Additional quantification, validation of electroporation, and gating strategies for microglia engulfment. Related to Figure 3.

(**A**) qRT-PCR for selected phagocytic pathway related genes in whole retina when neuronal SIRPα is removed. Values represent fold change in mRNA expression levels relative to the levels detected in controls for each gene following normalization to β-actin. n=3 control, 4 *SIRPα*^{NEURON} mice, unpaired *t*-test.

(**B**) Percent microglia with and without phagocytic cups in control, *SIRPα*^{NEURON}, and *SIRPα*^{MICROGLIA} microglia. n=8 control, 4 *SIRPα*^{NEURON}, 3 *SIRPα*^{MICROGLIA} mice. Data were compared using two-way ANOVA with posthoc Bonferroni correction.

(**C**) Representative confocal images following electroporation at P0 with plasmids overexpressing pCAG-GFP showing that *in vivo* electroporation mainly targets photoreceptors, with minimal expression in bipolar cells and Muller glia. Microglia and astrocytes are not targeted by electroporation. Scale bars, 50 μm.

(**D**) Validation of flow cytometry gating for Cx3cr1-GFP microglia shows that the majority of GFP^{+} cells are CD11b^{+}CD45^{low} microglia.

(**E**) Flow cytometry gating for microglial phagocytosis in Cx3cr1-GFP-positive microglia from *SIRPα*^{NEURON}*; Cx3cr1*$^{GFP/+}$ and *SIRPα*$^{F/F}$*; Cx3cr1*$^{GFP/+}$ retinas following incubation with yeast particles conjugated to pHrodo red.

Data from (**A**) were pooled from two independent experiments. Data from (**B**) were obtained from one experiment. All data are presented as the mean ± SEM. *p<0.05, ****p<0.0001, ns, not significant.

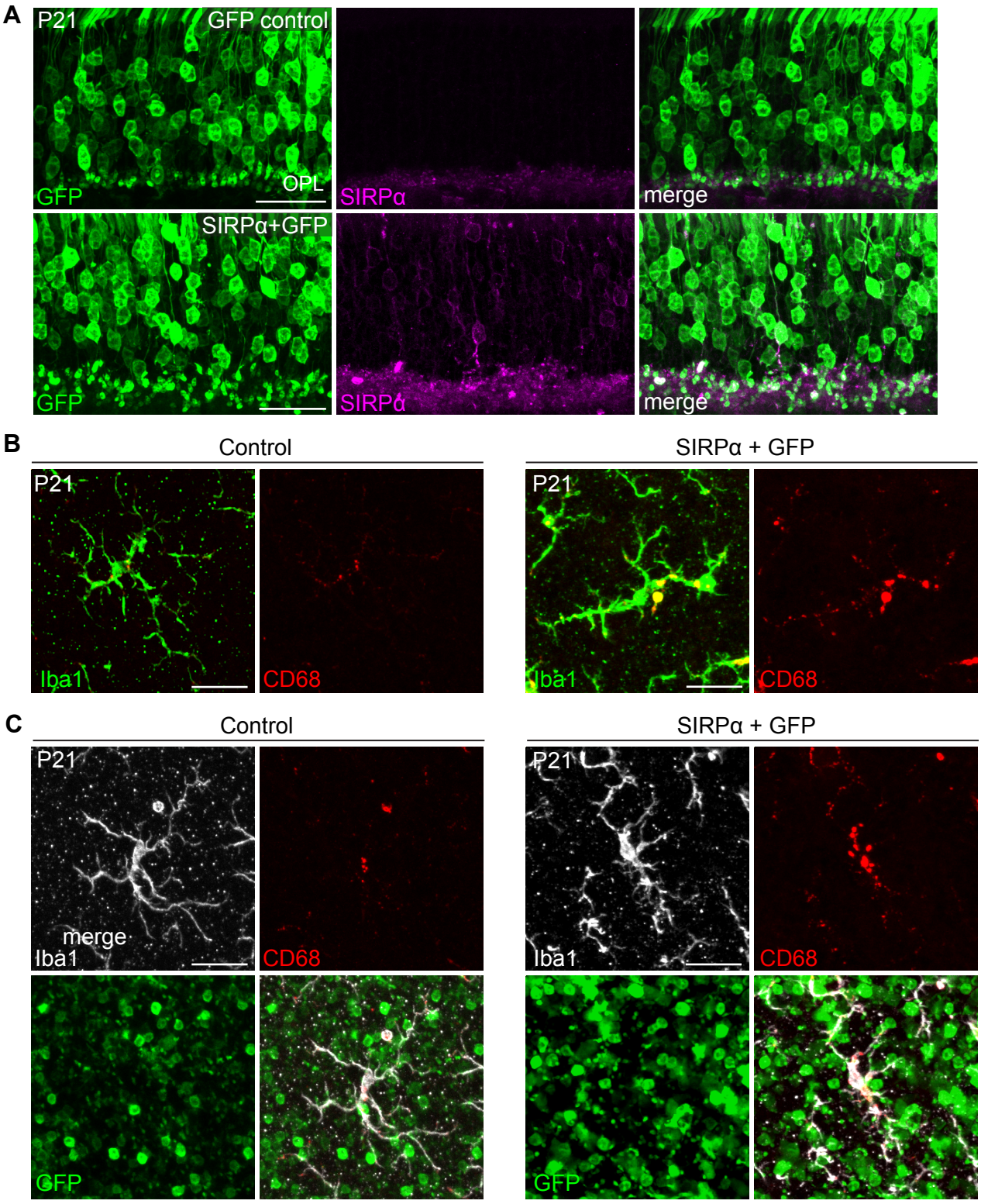

Figure S4. Validation of SIRPα overexpression following *in vivo* retinal electroporation. Related to Figure 5.

(**A**) Representative images of staining for GFP and SIRPα at P21 in WT retinas following electroporation with plasmids overexpressing GFP or GFP+SIRPα. Scale bars, 25 μm.

(**B**) Representative immunofluorescence images of 3D surface rendering in Figure 5B of Iba1-labeled microglia (green) containing CD68-labeled lysosomes (red) at P21 in WT retinas following electroporation with plasmids overexpressing GFP or GFP+SIRPα. Scale bars, 25 μm.

(**C**) Representative immunofluorescence images of 3D surface rendering in Figure 5L of Iba1-labeled microglia (gray) containing CD68-labeled lysosomes (red) and engulfed GFP-labeled neural material (green) at P21 in WT retinas following electroporation with plasmids overexpressing GFP or GFP+SIRPα. Scale bars, 25 μm.

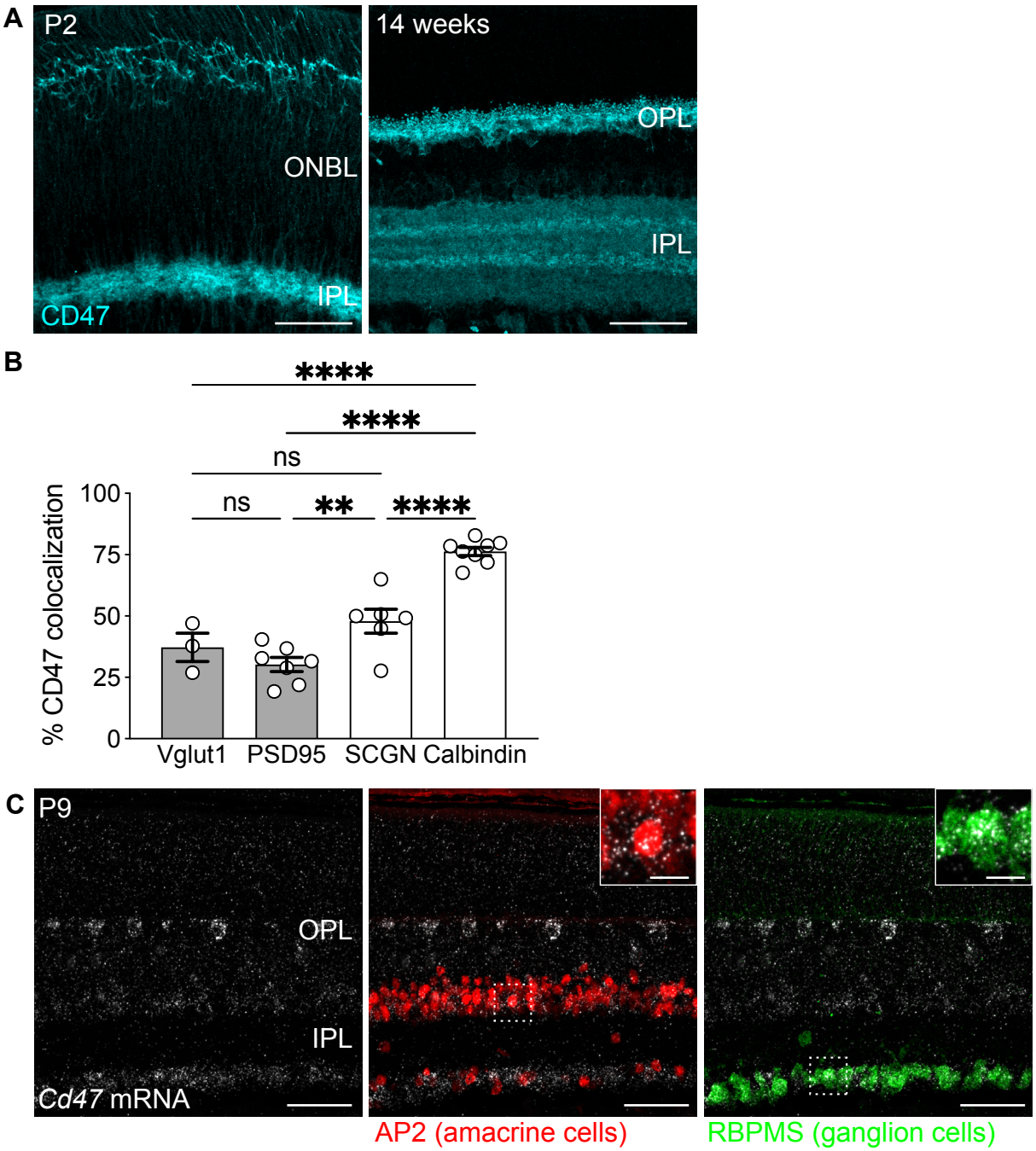

Figure S5. CD47 was expressed in postsynaptic cells, Related to Figure 6.

(**A**) Representative confocal images of CD47 expression in P2 and adult WT retinas. Scale bars, 50 µm.

(**B**) Quantification of the degree of colocalization between CD47 and presynaptic markers (Vglut1 and PSD95 for photoreceptor terminals) or postsynaptic markers (Calbindin for horizontal cell dendrites, SCGN for cone bipolar cell dendrites) at P14 in WT retinas using Manders' coefficients (MCC). n=3 for Vglut1, n=7 for PSD95, n=6 for SCGN, n=7 for Calbindin. Data were compared using two-way ANOVA with posthoc Bonferroni correction.

(**C**) Representative smFISH images of *Cd47* mRNA with IHC staining for inner retina neurons (AP2 for amacrine cells, red; RBPMS for ganglion cells, green) at P9 in WT retinas. Scale bars, 50 µm and 10 µm (insets).

Data from (**B**) were pooled from two to three independent experiments. All data are presented as the mean ± SEM. **p<0.01, ****p<0.0001, ns, not significant.

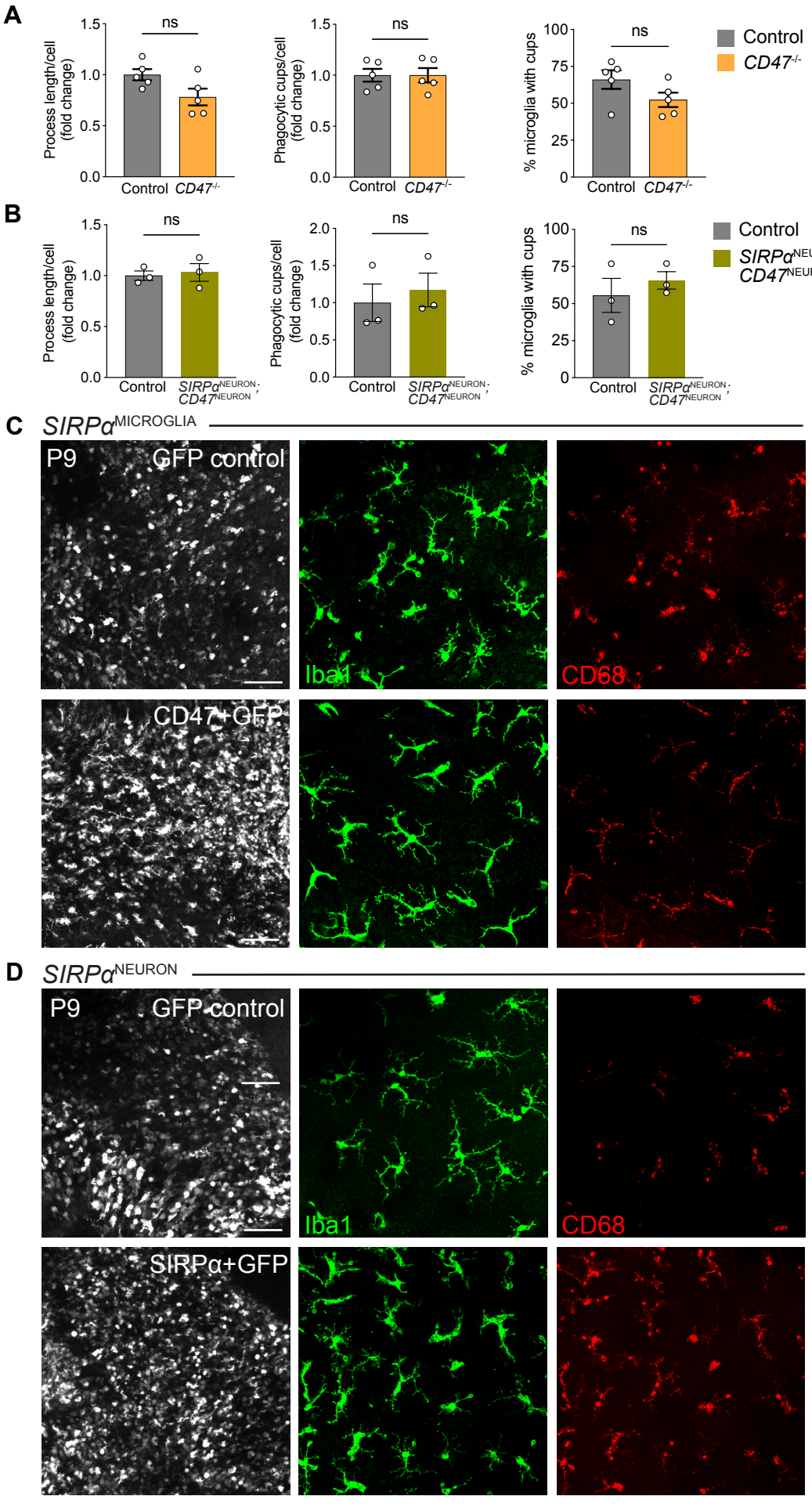
A
Process length/cell (fold change)
Phagocytic cups/cell (fold change)
% microglia with cups
ns
Control
CD47-/-
B
SIRPαNEURON, CD47NEURON
C
SIRPαMICROGLIA
P9
GFP control
CD47+GFP
Iba1
CD68
Process length/cell (μm)
Soma size (μm2)
CD68 fluorescence (A.U.)
GFP control
GFP +CD47
D
SIRPαNEURON
SIRPα+GFP
GFP +SIRPα
***
**

Figure S6. Neuronal SIRPα limited inhibitory CD47 signaling to microglia, Related to Figure 7.
(**A**) Additional quantifications of microglial morphology and levels of activation, including process length, number of phagocytic cups per cell, and percentage of microglia with cups in CD47 null mice and controls. n=5 mice per group, unpaired *t*-test.
(**B**) Additional quantifications of microglial morphology and levels of activation, including process length, number of phagocytic cups per cell, and percentage of microglia with cups in SIRPα/CD47 double knockout mice and controls. n=3 mice per group, unpaired *t*-test.
(**C**) Representative confocal images of GFP-expressing cells (white), Iba1$^+$ microglia (green), and CD68$^+$ lysosomes (red) in GFP and CD47+GFP electroporated *SIRPα*^{MICROGLIA} retinas, viewed in whole-mount. Scale bars, 50 μm. n=3 mice per group, unpaired *t*-test.
(**D**) Representative confocal images of GFP-expressing cells (white), Iba1$^+$ microglia (green), and CD68$^+$ lysosomes (red) in GFP and SIRPα+GFP electroporated *SIRPα*^{NEURON} retinas, viewed in whole-mount. n=6 control and 4 *SIRPα*^{NEURON} mice, unpaired *t*-test.
Data from (**B**) were obtained from one experiment. All other data were pooled from two to three independent experiments. All data are presented as the mean ± SEM. **p<0.01, ***p<0.001, ns, not significant.